



## A Comparative Study and Simulation of Reflecting Telescope Layouts Used in E-O Sensors of Remote Sensing Satellites

{F. El-Tohamy, M.E. Abdel Hady}\*

**Abstract:** The constraints of building a remote sensing satellite, with limited volume, weight and to acquire high image quality have resulted in innovative approaches to the design of the telescope as an essential and effective part of electro-optical (E-O) remote sensor performance parameters. The majority of the Earth observation satellites payloads are based on reflective telescopes due to their compact size, reduced weight of mirrors over lenses for the same entrance aperture diameter, in addition that reflective telescopes are free of chromatic aberrations. In this paper, the Cassegrain configuration layouts, as reflecting telescopes, and their preliminary design evaluation are presented. A comparison among these reflecting telescope layouts is executed using ZEMAX software package. Finally, a simulation of an optical telescope based on a proposed case study is developed using ZEMAX.

**Keywords:** remote sensing satellites, Cassegrain reflecting telescope, ZEMAX.

### 1. Introduction

An E-O remote sensor consists of three main parts, Figure (1), including the optical part, detector part, and the electronic part [1].

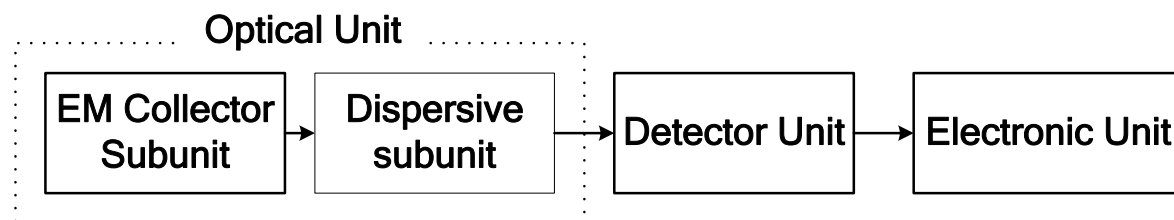


**Fig. (1) Main parts of a an E-O remote sensor**

The optical part consists of two basic units: the Electromagnetic (EM) collecting optics; i.e. the telescope, and the spectral dispersion unit. The telescope collects the EM radiation reflected/emitted from the scene under observation, and then focuses the collected radiation, directly or through the dispersion unit, into the detector part which is located at the focal plane of the telescope. According to the types of the used optical elements, optical telescopes used in E-O remote sensors may be classified into reflective, refractive or catadioptric type. In this paper, the Cassegrain configuration layouts, as reflecting telescope and their preliminary design evaluation are presented, also a comparative study between these reflecting telescope layouts is executed using ZEMAX software package [2] in section 2. A simulation of an optical telescope based on a proposed case study is developed using ZEMAX in section 3. Finally, section 4 presents a conclusion and an exclusive summary.

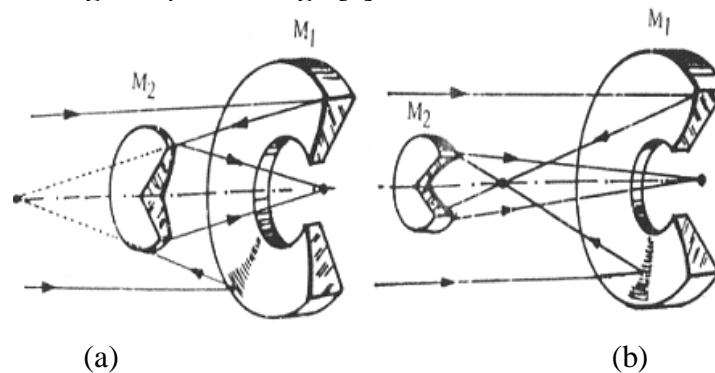
\* Egyptian Armed Forces, Egypt.

## 2. Reflecting Telescopes Used in E-O Remote Sensors

According to the types of the used optical elements, optical telescopes used in E-O remote sensors may be classified into reflective, refractive or catadioptric type [1]. Reflective telescopes consist entirely of mirrors. They are then totally achromatic and can operate at all wavelengths with very good transmittance, but its field of view is restricted by off-axis geometrical aberrations [3]. The limited field however can be enhanced by using refractive elements (called correctors). These correctors are introduced at the expense of having spectral transmittance that depends on the materials of the added refracting elements. The introduction of refractive correctors to a reflective telescope results in a catadioptric (reflection and refraction) telescope. Although refracting components have become common in wide-field optical systems, reflective telescopes are more advantageous than refractive ones, even with their limited field of view; due to their compact size, reduced weight of mirrors over lenses for the same entrance aperture diameter, in addition that reflective telescopes are free of chromatic aberrations.

### 2.1 Reflecting Telescope Configurations

The concept of the two-mirror telescope began to emerge with the postulation of both the Gregorian and Cassegrain type telescopes, Figure (2). The two layouts are primarily differentiated by their secondary mirrors. The Gregorian utilizes a concave secondary mirror placed beyond the focal point of the primary mirror while the Cassegrain utilizes a convex secondary mirror placed somewhat inside of the focus of the primary mirror. Both of these mirrors are designed such that the final focus takes place behind the primary mirror, which is perforated to allow the light to pass through [6].



Layout	Primary mirror $M_1$	Secondary mirror $M_2$
(a) Cassegrain telescope	Concave paraboloidal	Convex hyperboloidal
(b) Gregorian telescope	Concave paraboloidal	Concave ellipsoidal

**Fig. (2) Basic layouts of two-mirror reflecting telescopes**

The original postulation for the Cassegrain telescope (classical layout) has a concave paraboloidal primary mirror focusing its rays onto a convex hyperboloidal secondary mirror; Figure (2 a). This combination of aspheric curves yields excellent optical correction over moderate fields, where spherical aberration is eliminated. Optical designers modified the Cassegrain telescope design by fitting the asphericity between the two mirrors to control off-axis aberrations; practically speaking, optical optimization led designers of optical systems to modify the classical Cassegrain configuration into Ritchey-Chrétien and Dall-Kirkham telescopes [8].

The fundamental concept of the Ritchey-Chrétien is that the off-axis aberrations, resulting from wide field imaging, are reduced through aspheric optimization. In a classical Cassegrain there are two aberrations that are problematic: astigmatism and coma. The astigmatism component is quite small while the coma component is comparatively large. In the Ritchey-Chrétien design, the conic coefficient (aspherization constant),  $e$ , of the paraboloidal primary mirror;  $|e|=1$ , is altered into a hyperboloid;  $|e|>1$ , and the secondary mirror even is more hyperboloid, this can correct coma at the expense of astigmatism. But since astigmatism is so small it can be raised considerably before it becomes larger than the coma. The result is a two-mirror system optimized over a specific field of view. Therefore, while the classical Cassegrain layout is designed for high-resolution imaging over a small field, the Ritchey-Chrétien layout was developed for wide field imaging with an improved off-axis performance. All Cassegrain layouts of a given geometric design have the same field curvature whether they are a Ritchey-Chrétien, classical, and Dall-Kirkham or any other aspheric combination [3]. The Dall-Kirkham telescope has an ellipsoidal primary mirror,  $|e|<1$ , and a spherical secondary mirror,  $e=0$ . The advantage of the Dall-Kirkham lies in that the spherical secondary mirror is fundamentally easier for accurate fabrication, since figuring and accomplishing an aspheric surface; ellipsoidal, paraboloidal or hyperboloidal, is a sophisticated process in optics, and can result in a rough surface. Combined with the spherical secondary mirror and lightly aspherized primary mirror, the system is more accurately fabricated than any other compound two-mirror design. If properly designed and constructed, a Dall-Kirkham layout can deliver the finest images of any Cassegrain type telescope. The principle problem with the Dall-Kirkham design is that it does not correct well for comatic off-axis images [3]. It is worth mentioning that the majority of the Earth observation payloads utilize telescopes based on the Cassegrain configuration with its three layouts.

## 2.2 Preliminary Design of Cassegrain Layouts

The design of the three Cassegrain layouts shall be evaluated assuming the following:

- i. The remote sensor is operating in the visible band of the EM spectrum; at central wavelength  $\lambda = 0.55 \mu\text{m}$ .
- ii. The three layouts will have the same focal number  $F\# = 6.25$ ; ( $F\# = f/D$ ), where  $f$  is the effective focal length ( $f = 250 \text{ cm}$ ), and  $D$  is the entrance aperture diameter of the telescope ( $D = 40 \text{ cm}$ ).
- iii. Maximum field angle = 0.2 degree.

These assumed values shall be used to simulate the classical Cassegrain, Ritchey-Chrétien, and Dall-Kirkham telescope layouts using ZEMAX software package. Hence, the spot diagram (SD), modulation transfer Function (MTF), Optical path difference (OPD), and the transverse ray fan plot (TRFP) for the simulated layouts will be evaluated in order to select the appropriate layout to be applied for the case study.

The three layouts are optimized so as to form the best image over the entire field, rather than forming the best focus at the center. Each of the layouts given here will have a precise on-axis performance. Hence, the evaluation will be meaningful concerning the off-axis performance. Figure (3) and Table (1) summarize the simulation and design data of the three Cassegrain layouts.

Surf:	Type	Radius	Thickness	Class	Semi-Diameter	Conic
OBJ	Standard	Infinity	Infinity		Infinity	0.000000
STO	Standard	-128.644555 V	-47.239927 V	MIRROR	20.002714	-1.000000
2	Standard	-46.000000	66.393601 V	MIRROR	5.429243	-2.865700 V
IMA	Standard	Infinity			0.438926	0.000000

(a) Classical Cassegrain telescope data

Surf:	Type	Radius	Thickness	Class	Semi-Diameter	Conic
OBJ	Standard	Infinity	Infinity		Infinity	0.000000
STO	Standard	-138.000062 V	-52.348034 V	MIRROR	20.002529	-1.071293 V
2	Standard	-46.000000	60.332959 V	MIRROR	4.959779	-3.885356 V
IMA	Standard	Infinity			0.435950	0.000000

(b) Ritchey-Chrétien telescope data

Surf:	Type	Radius	Thickness	Class	Semi-Diameter	Conic
OBJ	Standard	Infinity	Infinity		Infinity	0.000000
STO	Standard	-138.000000	-52.348000 V	MIRROR	20.002534	-0.718175 V
2	Standard	-46.000000	60.338394 V	MIRROR	4.902798	0.000000
IMA	Standard	Infinity			0.451670	0.000000

(c) Dall-Kirkham telescope data

**Fig. (3) Results of simulation of the three Cassegrain layouts using Zemax****Table (1) Design data of the three Cassegrain layouts**

Design parameter	Cassegrain layout		
	Classical	Ritchey-Cretien	Dall-Kirkham
Primary mirror radius of curvature [cm]	-128.64	-138	-138
Primary mirror conic coefficient	-1	-1.07	-0.718
Secondary mirror radius of curvature [cm]	-46	-46	-46
Secondary mirror conic coefficient	-2.8657	-3.885	0
Primary-secondary mirrors spacing [cm]	47.24	52.35	52.35
Back focal length [cm]	19.1537	7.652	7.99
Total track length [cm]	66.3936	60.333	60.338

## 2.3 Design Evaluation of the Cassegrain Layouts

The evaluation of the previously designed layouts will be based on investigating their Spot Diagrams (SD), Modulation Transfer Function (MTF), Optical Path Difference (OPD), and Transverse Ray Fan Plots (TRFP).

### 2.3.1 Spot diagram evaluation

Figure (4) shows the spot diagrams of the previously designed Cassegrain layouts with respect to the theoretical Airy diameter for maximum field angle = 0.2 degree.

From figure (4) and Table (2), it is clear that the Ritchey-Chrétien layout has the smallest Airy disc diameter over the three layouts. Moreover, it has the smallest Geometric spot diameter with increasing field angles. Also, the three layouts suffer off-axis coma as the field angle increases.

### 2.3.2 Modulation transfer function evaluation

Figure (5) shows the MTF of the previously designed Cassegrain layouts. The MTF is a quantitative measure of image quality that describes the ability of an optical system to transfer an object contrast to its image. The MTF relates the working spatial frequency of the optics, expressed in line pairs per millimeter, to the percentage of the contrast measured from the original image. We shall briefly describe the concept of *MTF*. Practically the image of a point source is not a point, but is a disc (Airy disc). This is due to diffraction phenomena and aberrations of the optical elements of the imaging system. The intensity distribution of the image of the point source is called Point Spread Function (*PSF*). The Fourier transform of the *PSF* is known as the Optical Transfer Function (*OTF*). The amplitude of the *OTF* is *MTF*, which gives a measure of the decrease in the contrast modulation due to the imaging system as a function of spatial frequency [9]

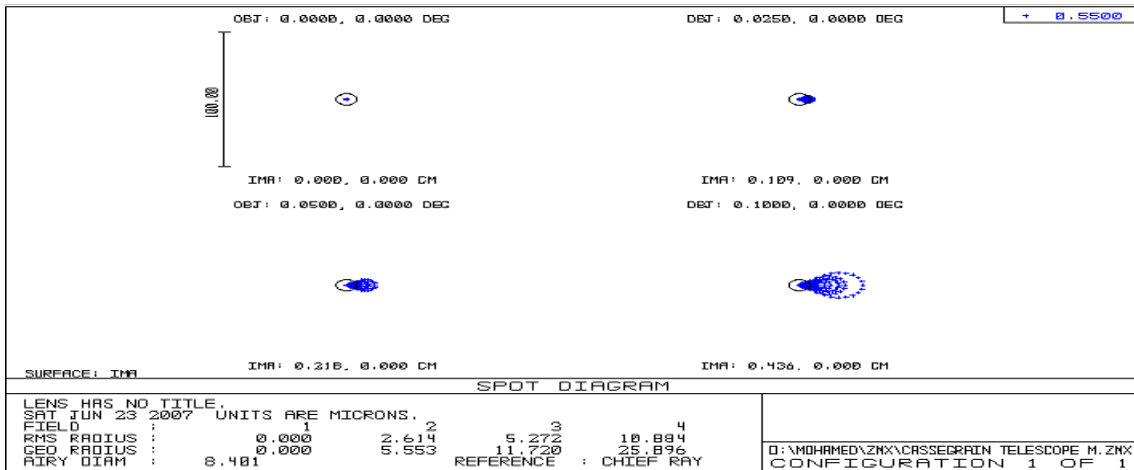
It is clear from Figure (5) that the Ritchey-Chrétien layout offers the best MTF.

### 2.3.3 Optical path difference evaluation

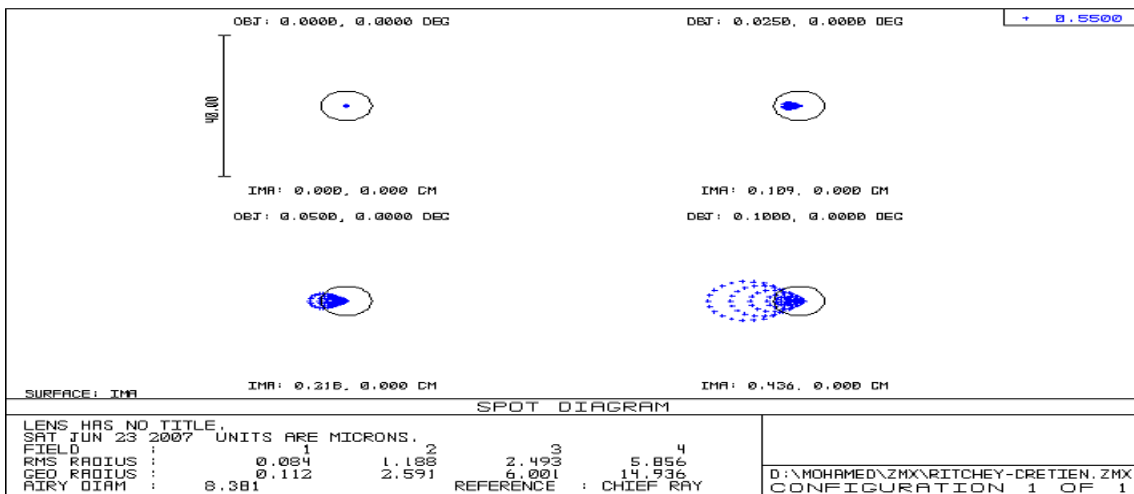
From Figure (6) and Table (3), the Ritchey-Chrétien layout has the smallest optical path difference over the three layouts for the whole field.

### 2.3.4 Transverse ray fan plot evaluation

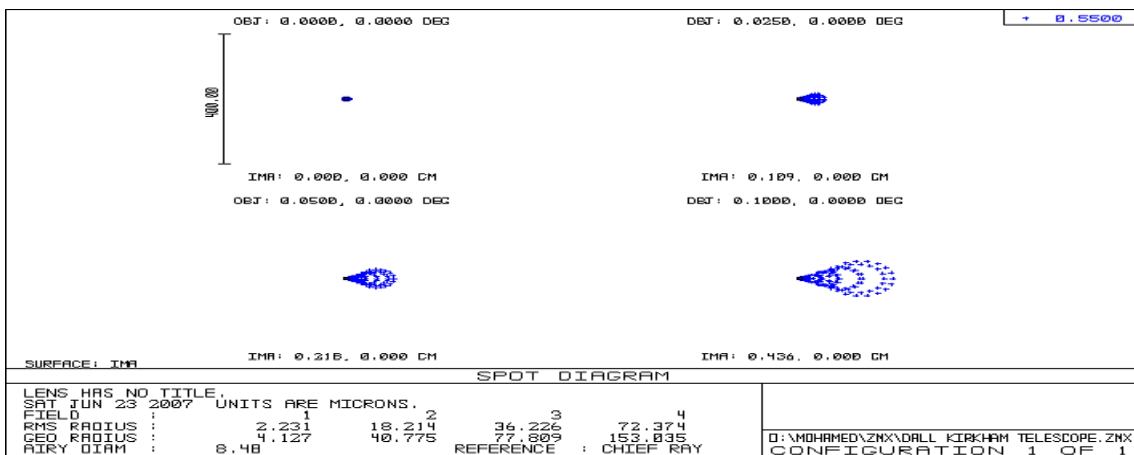
From Figure (7) and Table (4), the Ritchey-Chrétien layout has the smallest Spherical aberration over the three layouts for the whole field.



(a) Classical Cassegrain spot diagram

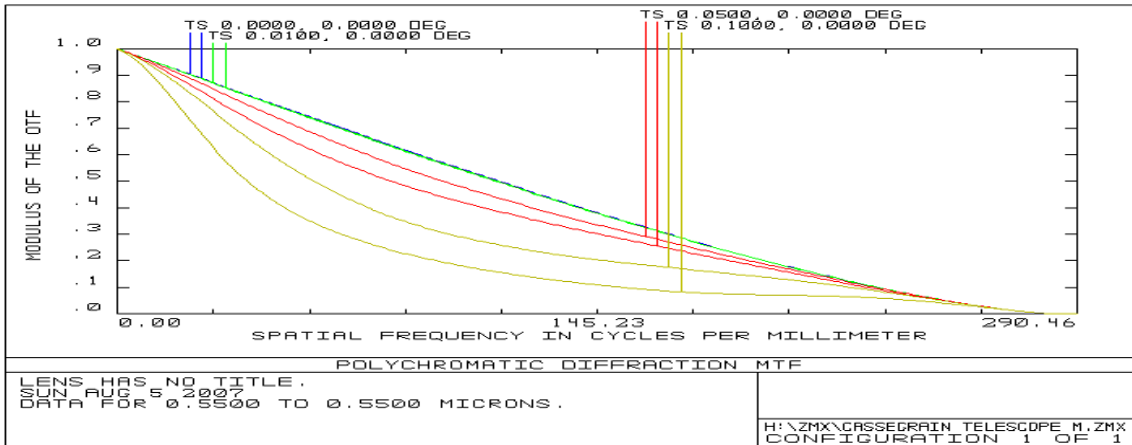


(b) Ritchey-Chretien spot diagram

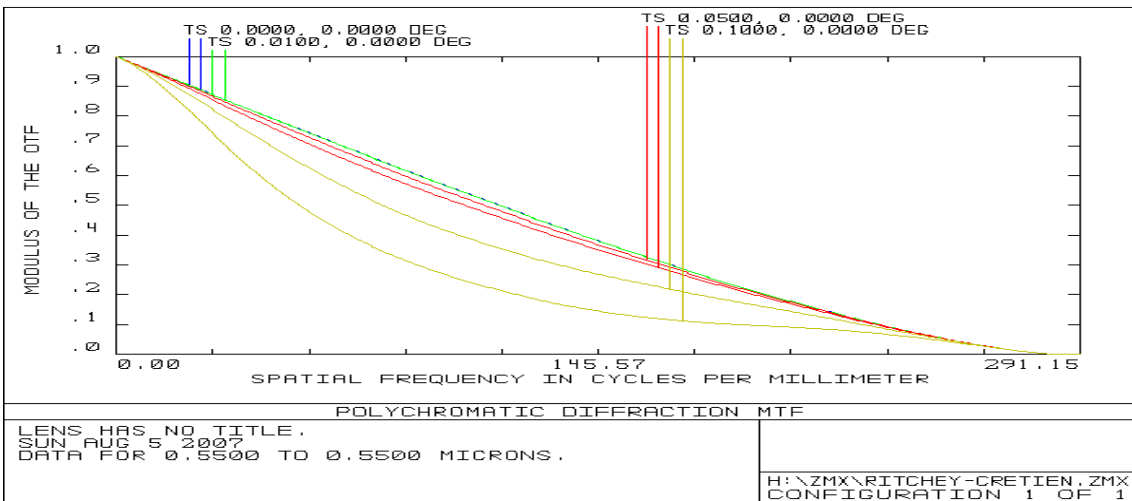


(c) Dall-Kirkham spot diagram

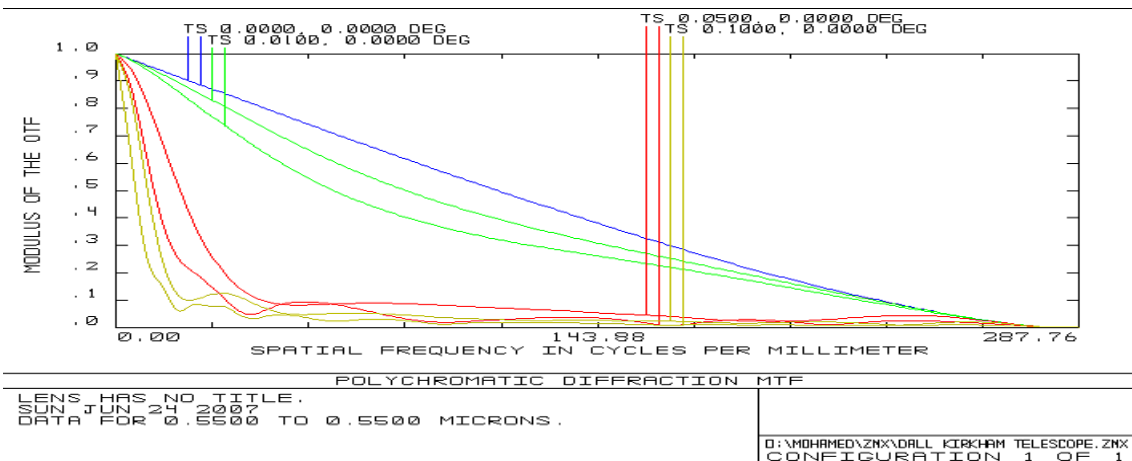
**Fig. (4) Spot diagram evaluation**



(a) Classical Cassegrain MTF

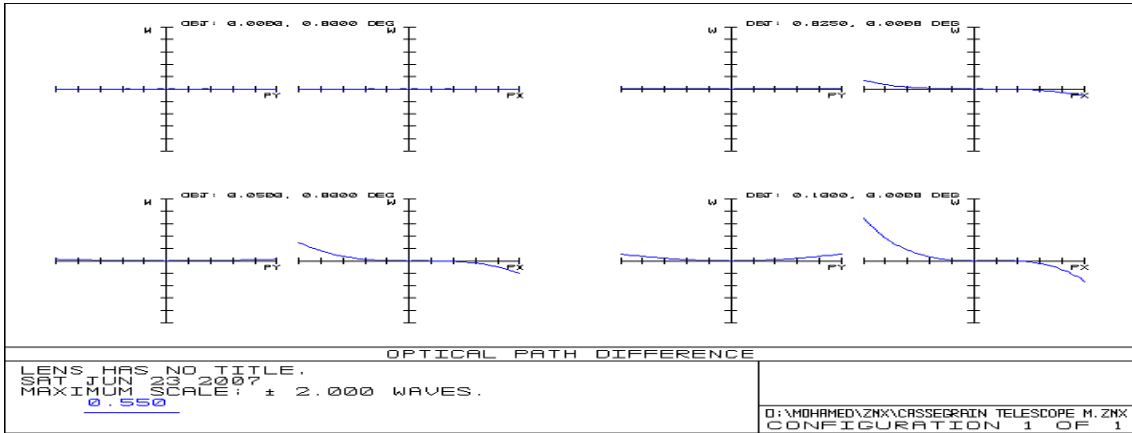


(b) Ritchey-Chrétien MTF

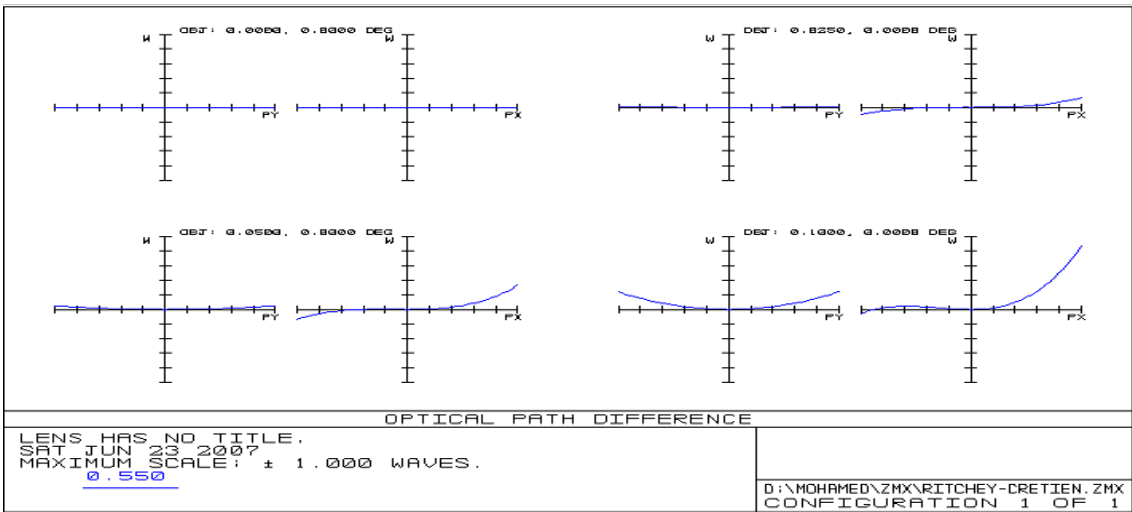


(c) Dall-Kirkham MTF

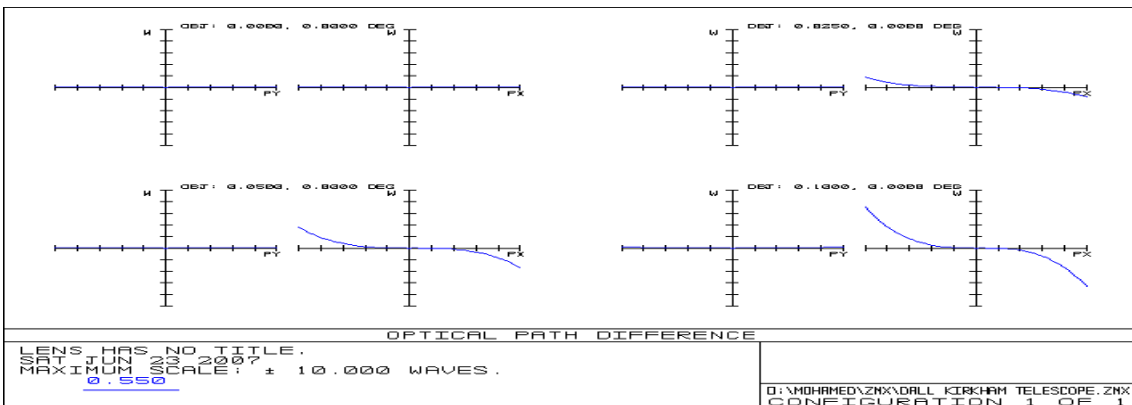
**Fig. (5) Modulation transfer function evaluation**



(a) Classical Cassegrain OPD



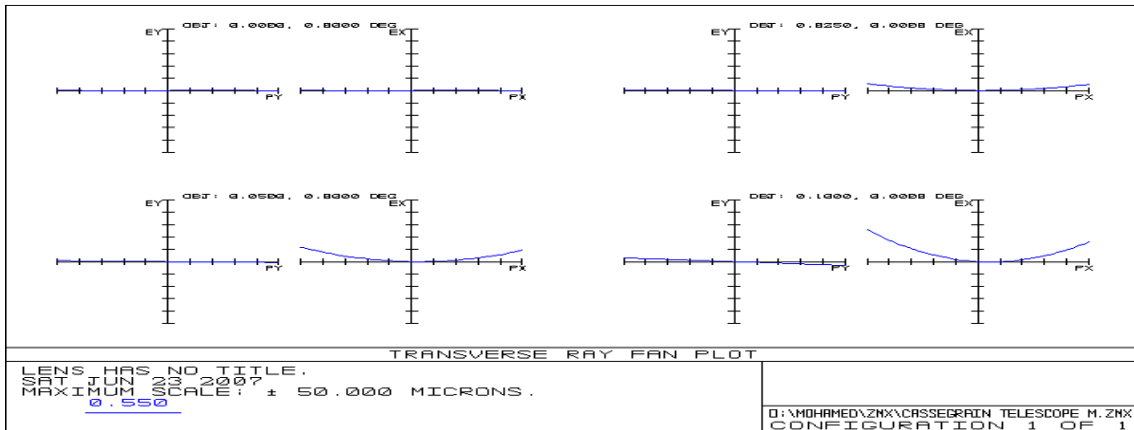
(b) Ritchey-Chrétien OPD



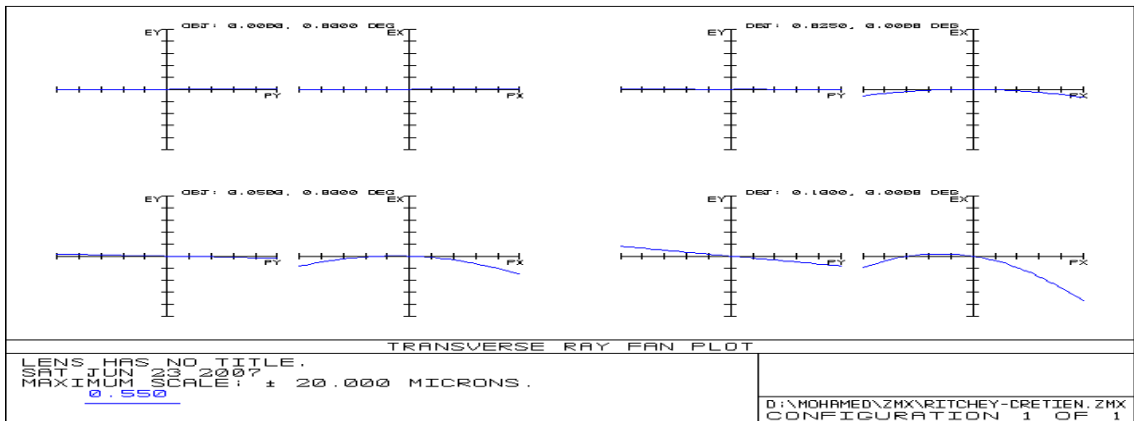
(c) Dall-Kirkham OPD

Fig. (6) Optical path difference evaluation

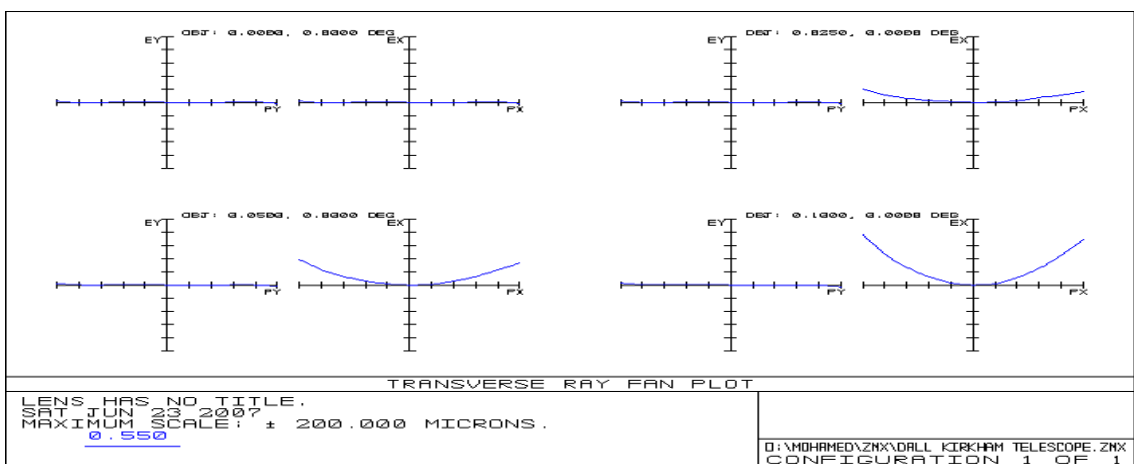




(a) Classical Cassegrain transverse ray fan plot



(b) Ritchey-Chrétien transverse ray fan plot



(c) Dall-Kirkham transverse ray fan plot

**Fig. (7) Transverse ray fan plot evaluation**

### 3. Case study

The first step in designing a telescope of a high resolution E-O remote sensor is the choice of its configuration which is mainly influenced by the limitations and performance requirements put upon the remote sensing satellite mission [8]. The second step in the design is SW telescope simulation [10]. From common software packages used in optics design and simulations are Zemax, Opti-cad, and Opal. In this section, Zemax SW package is utilized for a preliminarily simulation of a Ritchey-Chrétien telescope for an E-O sensor of a remote sensing satellite using pushbroom imaging technique, operating at the visible band, in a sun-synchronous orbit. The design parameters of the sensor are given in Table (5). The simulation of the Ritchey-Chrétien layout with Zemax software is performed to optimize its compactness, optical aberrations and MTF.

**Table (2) Spot size for Cassegrain layouts at different field angles**

Cassegrain layout/Airy disc diameter [ $\mu\text{m}$ ]	Geometric spot diameter at different field angles [ $\mu\text{m}$ ]			
	0.0 degree	0.05 degree	0.1 degree	0.2 degree
Classical / 8.401	0	5.553	11.72	25.896
Ritchey-Cretien / 8.381	0.004	2.591	6.001	14.931
Dall-Kirkham / 8.48	4.127	40.775	77.809	153.035

**Table (3) Optical path difference for Cassegrain layouts at different field angles**

Cassegrain Layout	OPD at different field angles [wave]			
	0.0 degree	0.05 degree	0.1 degree	0.2 degree
Classical	0	0.143	0.608	1.391
Ritchey-Cretien	0	0.07	0.343	0.865
Dall-Kirkham	0	0.716	3.693	7.217

**Table (4) Transverse ray fan plot for Cassegrain layouts at different field angles**

Cassegrain layout	Spherical aberration at different field angles [ $\mu\text{m}$ ]			
	0.0 degree	0.05 degree	0.1 degree	0.2 degree
Classical	0	5	10	25
Ritchey-Cretien	0	0.2	0.6	1.5
Dall-Kirkham	0	40	100	160

**Table (5) E-O sensor design parameters**

Sensor parameter	Symbol	Value	Sensor parameter	Symbol	Value
Altitude	$H$	600 Km	Spatial resolution	$GRD$	2 m
Central wavelength	$\lambda$	0.55 $\mu\text{m}$	Detector pixel size	$x$	7.5 $\mu\text{m}$
Number of detector pixels per array	$M$	2048	Swath width	$W$	4096 m

From the data given in Table (5), the telescope design parameters shown in Figure (8) are calculated as follows

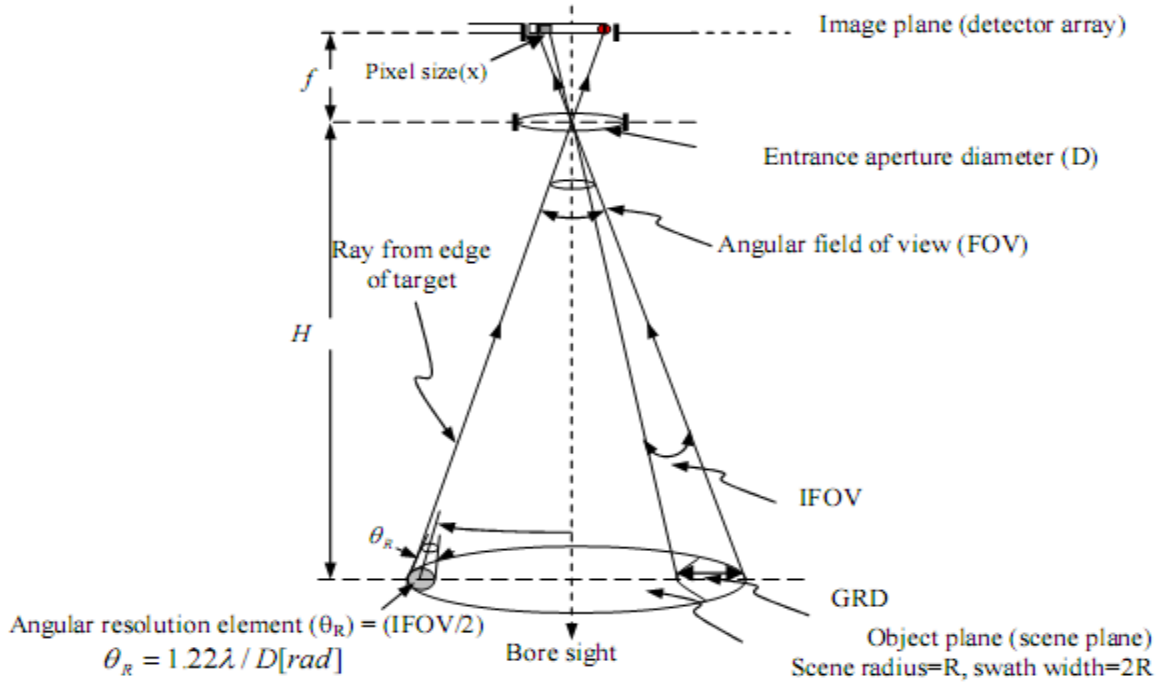


**Fig. (8) Design parameters of an electro-optical sensor**

i) Calculation of entrance aperture diameter ( $D$ ):

$$D = 2.44\lambda H / GRD = 2.44 \times 0.55 \times 10^{-6} \times 600 \times 10^3 / 2 = 40.26 \text{ cm}$$

ii) Calculation of effective focal length ( $f$ ):

$$\frac{f}{H} = \frac{x}{GRD} \quad , \quad f = \frac{xH}{GRD} = (7.5 \times 10^{-6} \times 600 \times 10^3) / 2 = 2.25 \text{ m}$$

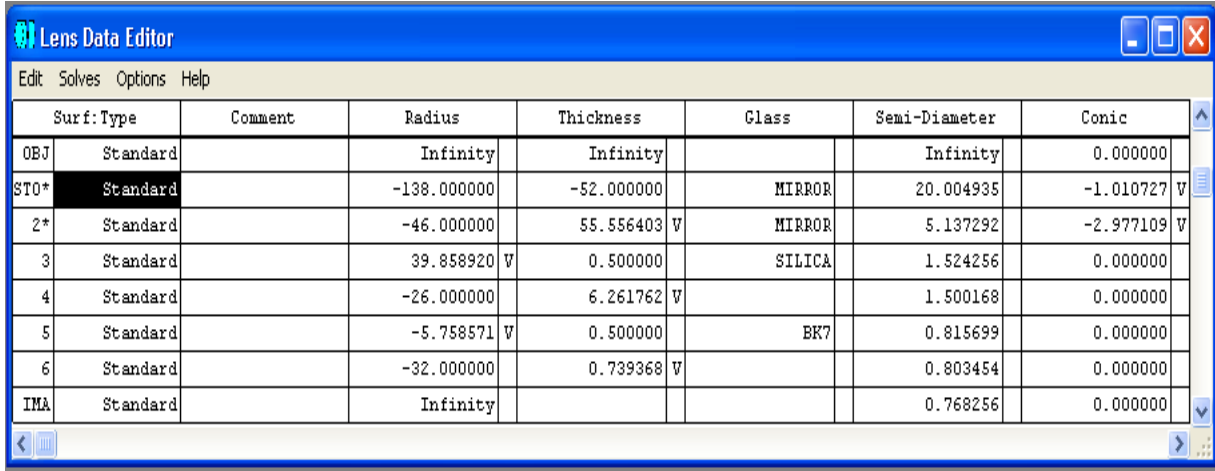
iii) Calculation of focal number ( $F\#$ ):

$$F\# = f / D = 2.25 / 0.4026 = 5.588$$

iv) Calculation of total field of view ( $\Omega$ ):

$$\tan(\Omega/2) = W/2H \quad , \quad \Omega = 2 \tan^{-1}(W/2H) = 2 \tan^{-1}(4096/1200000) = 0.391^\circ$$

From the design parameters of the proposed layout, ZEMAX optimized the telescope design parameters to give the best image with minimum optical aberrations and adequate MTF as shown in Figure (9) and Table (6).



Surf: Type	Comment	Radius	Thickness	Class	Semi-Diameter	Conic
OBJ	Standard	Infinity	Infinity		Infinity	0.000000
STO*	Standard	-138.000000	-52.000000	MIRROR	20.004935	-1.010727
2*	Standard	-46.000000	55.556403	MIRROR	5.137292	-2.977109
3	Standard	39.858920	0.500000	SILICA	1.524256	0.000000
4	Standard	-26.000000	6.261762		1.500168	0.000000
5	Standard	-5.758571	0.500000	BK7	0.815699	0.000000
6	Standard	-32.000000	0.739368		0.803454	0.000000
IMA	Standard	Infinity			0.768256	0.000000

**Fig. (9) Ritchey-Chrétien telescope with refractive correctors layout**

**Table (6) Simulated telescope design parameters**

Design parameter	Value	Design parameter	Value
Effective focal length [cm]	225	Working F#	5.621
Primary mirror diameter [cm]	40.26	Pr. mirror focal length [cm]	69
Secondary mirror diameter [cm]	9	Sec. mirror focal length [cm]	23
Primary-secondary mirrors spacing [cm]	52	Maximum field angle [degree]	0.391

The optimized data include the primary mirror conic coefficient, the secondary mirror conic coefficient, the radius of curvatures for the surfaces of the refractive correctors, and the final image location after the correctors as given in Table (7). The field curvature has been corrected by placing a doublet of plano-convex lenses beyond the primary mirror. The first lens is made up of silica, while the second lens is made up of BK7. In order to minimize the field curvature the lenses have to fulfill the Petzval condition,  $n_1 f_1 + n_2 f_2 = 0$  [4], where  $n_1$  and  $n_2$  are the refractive indices of the two lenses, and  $f_1$  and  $f_2$  are the focal lengths of the two lenses respectively

**Table (7) Telescope optimized design parameters**

Design parameter	Value	Design parameter	Value
Primary mirror conic coefficient	-1.0107	Secondary mirror conic coefficient	-2.977
Silica lens first surface curvature [cm]	39.858	Silica lens second surface curvature [cm]	-26
BK7 lens first surface curvature [cm]	-5.758	BK7 lens second surface curvature [cm]	-32
Telescope total track [cm]	63.5575		

The performance criteria of the proposed layout are shown in Figures (10), (11), (12) and (13).

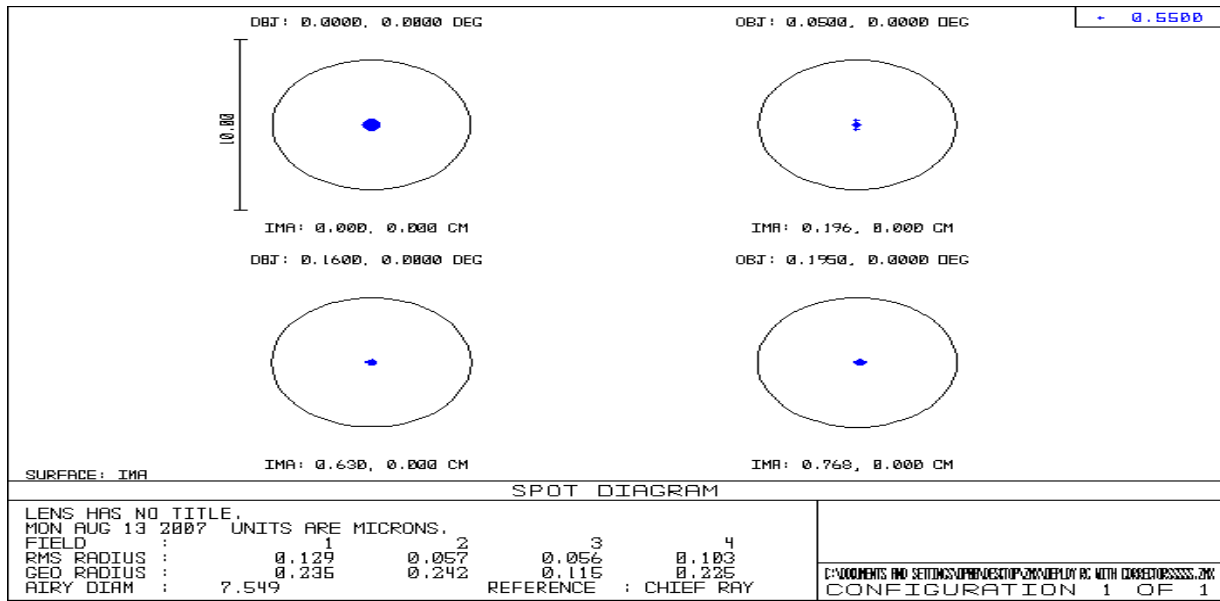


Fig. (10) Proposed Ritchey-Chrétien layout spot diagram.

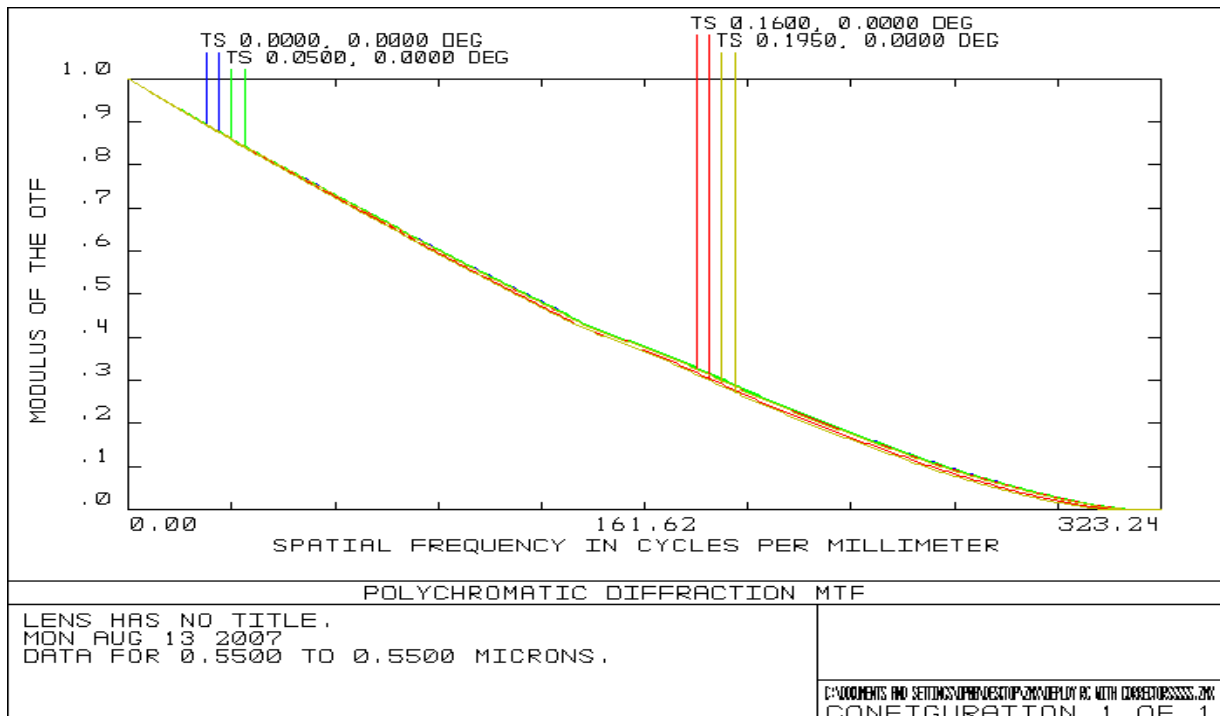
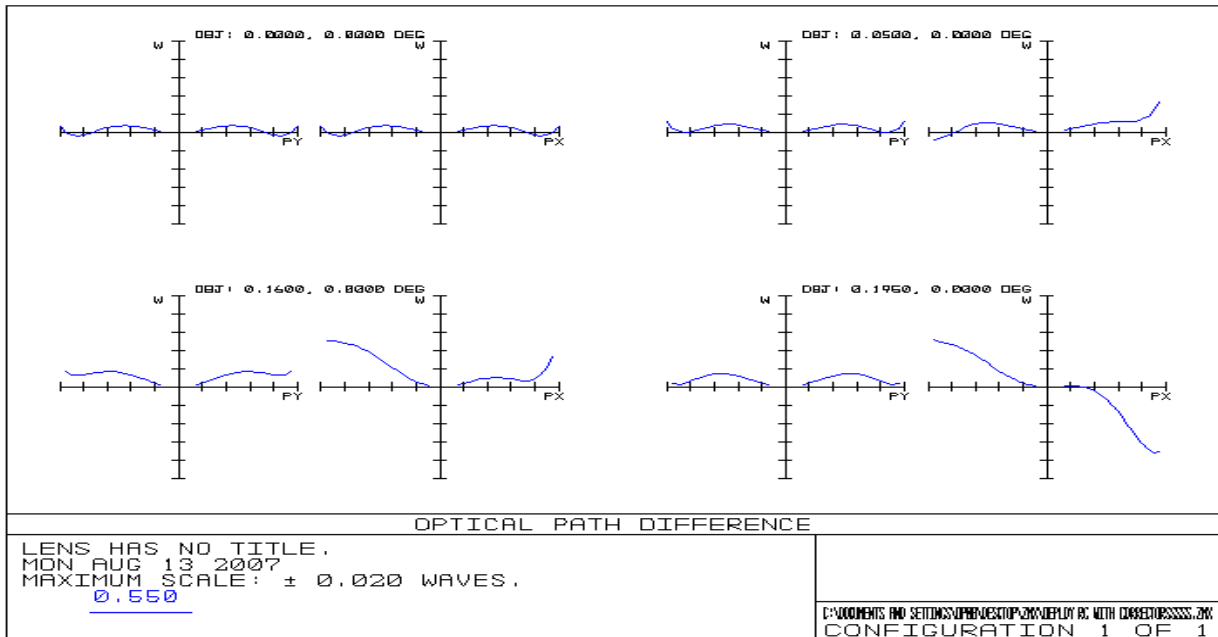
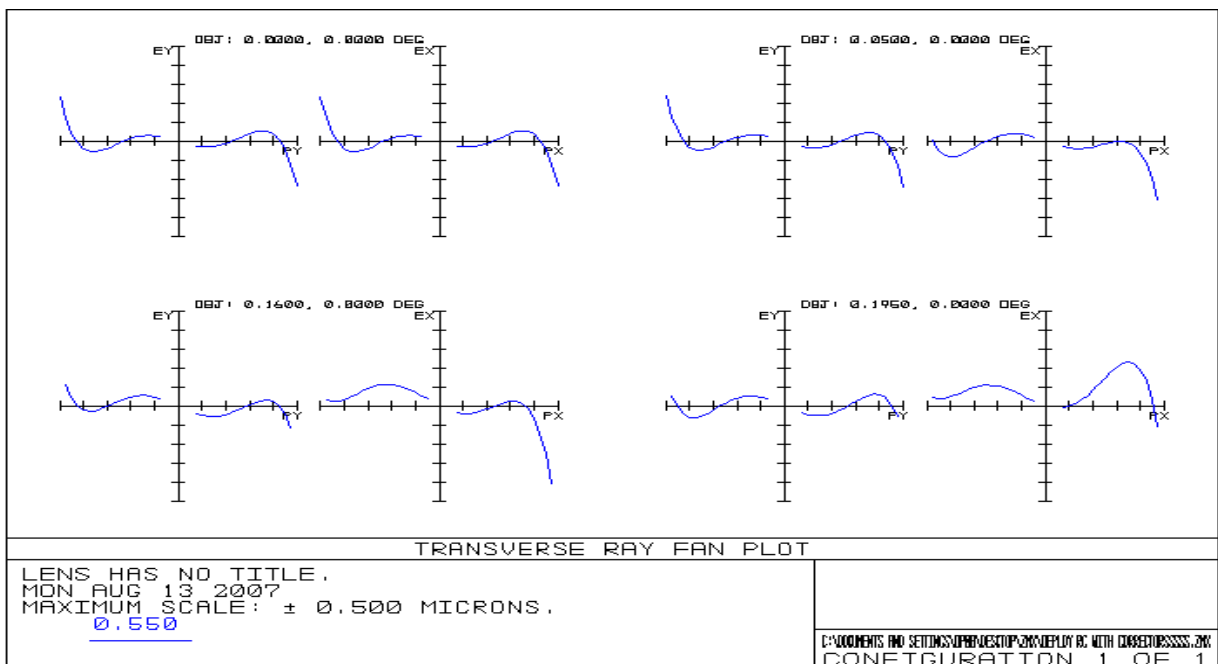


Fig. (11) Proposed Ritchey-Chrétien layout MTF.



**Fig. (12) Proposed Ritchey-Chrétien layout OPD**



**Fig. (13) Proposed Ritchey-Chrétien layout transverse ray fan plot**

Figure (10) shows that the image is well focused over the whole field with an Airy disc diameter of 7.549 [μm] giving a quality factor  $Q = 7.5 / 7.549 = 0.9935$  which is an acceptable value.

From Figure (11), the MTF at the working spatial frequency (66.67 line pairs/mm) is of an accepted value (MTF>70%).

Figure (12) emphasized that the telescope is diffraction-limited with maximum optical path difference of 0.0139 wave (less than 0.25 wave) for the entire field.

Figure (13) shows that the layout offers maximum spherical aberration of about 0.23  $\mu\text{m}$  for the entire field.

The simulated Ritchey-Chrétien layout reduces the spherical aberration and the coma, while the astigmatism aberration still present due to the non-spherical geometry of both mirrors.

## 5. Conclusion

In this paper, ZEMAX software package was used for a preliminary design, optimization of the design parameters and evaluation of the performance criteria for three reflecting telescope layouts used in electro-optical remote sensors. Also, a case study was held to verify an accepted performance parameters with optimum telescope size and reduced optical aberrations for a Ritchey-Chrétien layout fitted with refractive correctors. Finally, it is worth to mention that investigating a telescope configuration is a trade-off and iterative process between the telescope desired dimensions, based on the space mission requirements, and the quality of the produced images, controlled by the selected telescope layout that suppresses the optical aberrations and satisfies the desired performance parameters.

## References

- [1] Joseph, G., "Fundamentals of Remote Sensing", Universities Press, First Edition, 2003.
- [2] ZEMAX, Optical Design Program User,s Guide, Version 9.0, 2002
- [3] Smith, W. J., "Modern Optical Engineering", Second Edition, 1990.
- [4] Pedrotti, F. L., Pedrotti, L. M., and Pedrotti, L. S. "Introduction to Optics", Prentice-Hall International, Inc., Third Edition, 2007.
- [5] Smith, W. J., "Modern Lens Design", McGraw-Hill, Inc., First edition, 1992.
- [6] Born, M., Wolf, E., "Principles of Optics", Cambridge University Press, Seventh (Expanded) Edition, 1999.
- [7] Guenther, R. , "Modern Optics", John Wiley & Sons, Inc., 1990.
- [8] Larson, W. J., and Wertz, J. R., "Space Mission Analysis and Design", W .J. Larson and Microcosm, Inc., Second Edition, 1992.
- [9] Williams, C. S., Becklund, O. A., "Introduction to the Optical Transfer Function", John Wiley & Sons, Inc., 1995.
- [10] Pica, G., "High Resolution Deployable Telescope for Satellite Application", Proceedings of Spie's Remote Sensing, Europe 2003.